LAWRENCE
LIVERMORE
NATIONAL
LABORATORY

UCRL-JRNL-217421

Direct Observations of Rapid Diffusion of Cu in Au Thin Films using In-Situ X-ray Diffraction

J. W. Elmer, T. A. Palmer, E. D. Specht

November 30, 2005

Journal of Vacuum Science and Technology - A

Direct Observations of Rapid Diffusion of Cu in Au Thin Films using In-Situ X-Ray Diffraction

by:

J. W. Elmer and T. A. Palmer
Lawrence Livermore National Laboratory, Livermore, CA, 94551, USA

E. D. Specht
Oak Ridge National Laboratory, Oak Ridge, TN, 37831, USA

Keywords
Synchrotron Radiation, Interdiffusion, Grain Boundary Diffusion, Thin Films, Binary Alloys, Activation Energy

Abstract

In-situ x-ray diffraction was performed while annealing thin-film Au/Cu binary diffusion couples to directly observe diffusion at elevated temperatures. The temperature dependence of the interdiffusion coefficient was determined from isothermal measurements at 700ºC, 800°C, and 900ºC, where Cu and Au form a disordered continuous face centered cubic solid solution. Large differences in the lattice parameters of Au and Cu allowed the initial diffraction peaks to be easily identified, and later tracked as they merged into one diffraction peak with increased diffusion time. Initial diffusion kinetics were studied by measuring the time required for the Cu to diffuse through the Au thin film of known thickness. The activation energy for interdiffusion was measured to be 65.4 kJ/mole during this initial stage, which is approximately 0.4x that for bulk diffusion and 0.8x that for grain boundary diffusion. The low activation energy is attributed to the high density of columnar grain boundaries combined with other defects in the sputter deposited thin film coatings. As interdiffusion continues, the two layers homogenize with an activation energy of 111 kJ/mole during the latter stages of diffusion. This higher activation energy falls between the reported values for grain boundary and bulk diffusion, and may be related to grain growth occurring at these temperatures which accounts for the decreasing importance of grain boundaries on diffusion.

Introduction

Copper and gold are high conductivity metals used widely in the semiconductor industry and elsewhere [1]. Thin Au coatings are sometimes used on Cu substrates to prevent oxidation of the Cu and to enhance electrical conductivity, but these thin coatings can diffuse into the copper substrate over periods of time, even at moderately low temperatures. Numerous studies have investigated the diffusion of Au in Cu using different techniques such as tracer diffusion [2], high resolution electron microscopy [3], x-ray diffraction [4], and Rutherford back-scattering [5, 6]. The effects of grain boundaries and other defects have been investigated and are of particular importance since they accelerate the diffusion rate [7-9].

At elevated temperatures, Cu and Au are mutually soluble and form a melting point minimum at 910ºC [10], which makes this alloy combination useful to join the materials together through a eutectic-type bonding method. However, due to the high diffusivity of Au in Cu at elevated temperatures, thin-films of gold may diffuse into the copper during heating to the bonding temperature, thus altering both the temperatures at which the liquid first forms and the widths of the joints produced [11]. This study was undertaken to further investigate the diffusion of Au into Cu using a synchrotron based x-ray diffraction technique in order to determine the temperature dependence of the interdiffusion that occurs at elevated temperatures in Au-Cu thin films. The in-situ synchrotron studies presented here are particularly useful in that they directly track the initial rapid diffusion that takes place as the thin films intermix, as well as follow the interdiffusion that takes place at longer times. The real-time information gathered from these experiments reveals information about the kinetics and the mechanisms responsible for the interfusion that takes place.

Experimental Procedures

Sample Preparation

The thin film samples were prepared by first depositing high purity Cu onto a stainless steel substrate. A high purity Au layer was then deposited on top of the Cu layer to complete the composite sample. This arrangement allowed carefully controlled layers of Au and Cu to be deposited onto the stainless steel substrate so that the coated bar could be resistively heated to the required temperatures. The stainless steel substrates consisted of rectangular bars that measured 100 mm long, 4.75 mm wide and 2 mm thick. These samples were machined from AISI type 304 stainless steel that was originally acquired in 100 mm diameter bar stock. Chemical analysis was performed on the stainless steel showing it to contain (wt. %): 18.44% Cr, 10.71% Ni, 0.019% C, 0.053% N, 1.67% Mn, 0.04% Mo, <0.005%Nb, 0.46% Si, 0.04% V, 0.04% Cu, 0.02% Co, 0.016%S, 0.015% P, balance Fe (68.5%). One face of the stainless steel bar (4.75 mm x 100mm) was mechanically lapped to a finish of 0.1 μm rms in preparation for the coatings. Prior to applying the coatings, the lapped stainless steel bar was first cleaned with acetone and then wiped with ethanol to remove machining oils and contaminants.

The coatings were deposited on non-heated substrates using planar magnetron sputtering in a vacuum chamber with base pressure in the 10^{-7} torr range. Five samples were prepared, all coated together to provide identical starting conditions. The lapped and cleaned stainless steel surface was first cleaned by ion milling with argon ions. They were then coated with a thin (nominally 10.5 nm) flash of 99.995wt% Ti using one sputtering source in order to assist the adhesion of the Cu to the stainless steel. This surface was then co-sputtered with Ti and 99.99wt% Cu from a second sputtering source to provide a thin (nominally 10.5 nm) transition from the stainless steel to the pure Cu layer without breaking vacuum. The Ti source was then turned off to deposit a 35 μm thick Cu layer on top of the Ti/Cu layer during a16 hr run. The

system was vented, the sputter target was changed and the sample stage was repositioned to sputter deposit the Au layer.

After repositioning the substrates and installing the Au target, the system was pumped down to a base pressure of $3.0X10^{-7}$ torr. The Cu-coated bars were ion-milled for 30 s in high purity argon at 3 sccm and a pressure at $2.4X10^{-3}$ torr. The Au layer was then deposited from a 99.995wt% target during a 1 hr 42 min run at a deposition rate of 350 Å/min, yielding an average thickness of 3.8 μm. The argon gas flows and pressures for deposition were 20 sccm flow /10mt pressure ($9.1x10^{-3}$ chamber).

The thickness of the resulting Cu and Au layers were determined from step height measurements made at the edges of each coating using an Ambios XP2 profilometer. The Cu and Au heights were able to be individually measured since the Cu layer was masked to be 1.5 inch long and the Au layer was masked to be 1.0 inch, leaving clean steps at each interface. Figure 1 shows a photograph of one of the completed samples, where the 1 inch wide gold layer is clearly visible in the center of the 1.5 inch long Cu layer. The thickness of the Au layers of the 5 samples was measured to be 3.82 ± 0.47 μm, and that of the Cu layer was measured to be 35.4 ± 1.00 μm. Variations in the thicknesses of the layers were present due to the relatively large sputter area. These values were individually recorded for each sample and used when detailed calculations were required.

In-Situ X-Ray Diffraction Experiments

Experiments were performed by heating sputter coated samples to a given temperature while observing the x-ray diffraction patterns using real time x-ray diffraction. The x-ray diffraction measurements were performed on the UNICAT beam line BM-33-C at the Advanced Photon Source (APS) using a 30 keV x-ray beam from a ring current of 100 mA. This beam line was set up with a water cooled Si (111) monochromator, and the beam was focused and sized to

dimensions of 1 mm wide by 0.25 mm high using a dynamically bent Si crystal and collimator slits. The X-ray detector, manufactured by Roper Scientific (A99k401, RS/Photometrics), focuses light from a scintillating screen onto a Peltier cooled 16-bit CCD using a tapered fiber optic bundle. The effective pixel size of the 1024 x 1024 array is 60 μm. A schematic of the experimental setup is shown in Fig 1, which is further described elsewhere [12, 13].

The test coupons were clamped into a water-cooled copper fixture that allows high electrical currents to be passed through them. Rapid heating of the samples was performed by resistive heating, while rapid cooling was accomplished using water cooled grips. The direct resistive heating of Cu or Au would require prohibitively high currents of approximately 1000 amps, due to the high thermal conductivity and low electrical resistivity of these materials. The use of thin samples would reduce the required heating current, but would lead to sagging as the samples are heated. This problem was overcome by coating a stainless steel substrate, which has higher electrical resistivity than Cu, with a thin layer of Cu and then depositing the Au layer on top of the Cu layer. Heating to 900°C requires approximately150 A, which is easily accomplished with this setup.

The temperature of the sample was monitored during the experiment using type-S (Pt/Pt-10%Rh) thermocouples which were spot welded on the back side of the sample directly below the x-ray impingement point. A Eurotherm 818 temperature controller, a Eurotherm 425A power thyristor, and a Trindl RT300 transformer were used to control the AC current passing through the sample so that pre-programmed thermal cycles could be followed in a controlled manner. The sample assembly was enclosed inside an environmental chamber that was pumped down to the millitorr level using a turbomechanical pump in order to minimize oxidation of the sample during high temperature runs. The heating power supply is capable of producing 300 Amps at 6V and can heat the stainless steel sample up to temperatures as high as 1400ºC, at rates

as high as 50°C/s.

While the sample is being heated, the x-ray beam impinges on the top surface of the sample at a 6 deg angle of incidence. This angle provided an x-ray penetration through the Au layer and also into the Cu layer at the beginning of the test, allowing both phases to be internally calibrated before any diffusion takes place. The diffracted beams were collected using a CCD detector that was placed 330 mm behind the sample. One of the initial x-ray diffraction patterns is presented in Fig. 2. In this figure, the Debye arcs of the diffracted beam are shown at room temperature for a 2-theta range from 17.0 deg to 34.8 deg for the 30 keV x-ray beam.

During the experiment the detector captures the x-ray data by integrating the diffracted beams over a 1s exposure. Another 2s is required to clear the data from the CCD detector and transfer it to the computer, thus it is possible to capture a complete diffraction pattern approximately every 3s with this arrangement. The detector read-out was accelerated by a 2x2 binning of the pixels. An advantage of the 2D detector is that a larger number of grains satisfy the diffraction condition than do for a conventional theta/2-theta scan, so statistically valid diffraction data can be collected for more coarse-grained samples.

To calibrate the x-ray detector, the lattice parameter of pure OFHC copper was measured at room temperature using a conventional Cu K_α x-ray diffraction system. The x-ray diffraction patterns from the in-situ synchrotron studies were then fit to this lattice parameter by selecting five points along each of three Debye arcs gathered from the initial diffraction pattern for each run. Finally, the sample-detector distance, the position of the center of the arcs on the detector, and the magnitude and orientation of the detector tilt are varied to minimize the difference between the d-spacing at the selected points as calculated from these detector patterns and that calculated from the lattice parameters. Using this calibration, the Debye arcs are converted into a 1-D plot showing diffracted beam intensity versus d-spacing using Fit-2D software [14, 15].

This software integrates the diffracted beam intensity for each arc over the entire 2-D areal array, creating an intensity versus d-spacing plot like the one shown in Fig 3.

Results

General Observations and Initial Sample Condition

The design of the samples was such that the Au film was thin enough to allow penetration of the 30keV x-rays through it and into the Cu below. Thus the initial diffraction patterns, before any diffusion had taken place, contain both Au and Cu peaks. Figure 3 shows one of the initial diffraction patterns indicating that three sets of peaks are present for each element: fcc(111), fcc(200) and fcc(220). In addition, a partial Au fcc 311 peak appears at the lowest d-spacing location. The large shift in the positions of the diffraction peaks for the two elements results from the 12% difference in their lattice parameters which are known to be 4.0783Å for Au, and 3.6153Å for Cu at room temperature [16]. Note that the Cu peaks are much lower in intensity than the Au peaks in the initial diffraction pattern due to the attenuation of the x-rays as they pass through the Au layer.

During heating, all of the peaks shift to higher d-spacings due to the thermal lattice expansion effect. The amount of lattice expansion is higher for Cu, which has a reported coefficient of thermal expansion (CTE) of 17.0×10^{-6}/ºC, than for Au, which has a reported CTE of 14.1×10^{-6}/ºC [17]. Prior to interdiffusion of the Au and Cu, additional shifts in the peak positions may occur as any residual stress in the films, induced during the sputter deposition process, thermally relaxes as the sample heats.

When the samples reach the annealing temperature, interdiffusion of the Au and Cu takes place as a function of annealing time. Since diffusion of Cu into Au is faster than that of Au into Cu [17], it is expected that the first effect observed will be Cu diffusing into the thin Au layer, decreasing the Au lattice parameter to that of the intermixed solid solution (Au/Cu). Each pair of

Cu and Au/Cu diffraction peaks should eventually homogenize into one peak at long annealing times, and have a d-spacing between those of the initial peaks. By monitoring the changes in peak position with in-situ x-ray diffraction during the elevated isothermal holding times, these changes and the kinetics of interdiffusion can be monitored in real time.

Elevated Temperature Experiments

The x-ray diffraction experiments were performed by heating the samples to predetermined temperatures of 700, 800 and 900ºC, at a constant heating rate of 21ºC/s. Diffraction patterns were captured every 3s as described above for the first several min of the run where the peak shape and positions were changing the most, then every 10s afterwards to minimize the amount of data stored. The samples were held at their respective temperatures for times up to 8 hours to produce long range diffusion in the thin films.

The evolution of peak positions for each temperature are plotted in Fig. 4a-c, which compares the Au(200) and Cu(200) d-spacings for the initial 200s of the heating cycle. Superimposed on each figure is the temperature profile throughout the heating cycle. It is clear in these figures that the d-spacings for the Cu peaks continue to increase up to the point where the isothermal hold temperature is reached, and that those of the Au peaks begin to decrease before the hold temperature is reached, due to diffusion of Cu into the thin Au film. The Au peaks begin to shift to lower d-spacings at approximately the same time. This is because the transformation begins before any of the isothermal temperatures are reached, and because the heating rates are the same for all three experiments. The point where the Au peaks begin to shift to lower d-spacings corresponds to a temperature of approximately 650ºC for each of the experiments.

Once the Au peaks begin to shift to lower d-spacings the rate of change is rapid at first but decreases throughout the remainder of the experiment. The total change in peak positions is

dramatic, whereby the position of the initial Au peak approaches that of its corresponding Cu peak at large diffusion times. Fig. 5 shows this change for the 800ºC anneal where the initial diffraction pattern is superimposed on the final diffraction pattern after an annealing time of 2 hours. The initial diffraction pattern contains both Au and Cu peaks whereas the final diffraction pattern shows only one peak which is the endpoint of the intermixed Cu/Au film. The final peak has a higher intensity than the initial Au peak, and its position moves to a location near the initial Cu peak. Since the initial thickness of the Cu layer was approximately 10 times that of the Au layer, the final average composition of the interdiffused coatings is closer to that of Cu than Au. Similar results were found at the other two temperatures, though the amount of time required to homogenize the films was different, decreasing with increasing temperature as expected.

Discussion

Initial Stages of Interdiffusion

Because the diffraction profiles are qualitatively different early and late in the interdiffusion process, different analysis techniques must be used. Early diffusion rates are compared based on the time for the Au peak to sharpen, indicating that a uniform composition has developed in the Au layer of known thickness at the surface of the sample. Late diffusion rates are compared based on the time required for the near-surface region to reach various compositions.

During the initial stages, interdiffusion of Au and Cu occurred rapidly starting at temperatures of approximately 650ºC and was accompanied by a corresponding change in the profiles of the Au peaks. Figure 6 shows the peak shift for the (220) reflections taken at 3 s intervals during the 800°C run where rapid diffusion is taking place. These superimposed profiles show the initial interdiffusion stage from t=36 s to t=57 s, where a Cu-rich shoulder

builds up and grows on the low d-spacing side of the Au peak. The annealing temperature of 800°C is reached midway between this transition at t=48 s where the Cu(220) reflection stabilizes its peak position but the Au peak continues to decrease in d-spacing with further annealing. The growth of the shoulder on the Au peak is rapid and distinct, indicating that Cu is diffusing into the bottom of the 3.8μm thick Au layer, creating this shoulder. Eventually one single Au/Cu peak is formed, and this peak continues to move to lower d-spacing values with increased annealing time. Similar rapid transitions were observed in experiments performed at 700ºC and 900ºC.

The peak broadening observed in Fig. 6 results from the different lattice parameters of the Cu and Au phases. In addition, since both elements are fcc and do not form ordered compounds at these annealing temperatures [10], the peak broadening should occur in a continuous manner through substitutional diffusion of Cu and Au through the fcc lattice. Figure 7 plots the measured width of the (111) reflections during each of the three runs for the first 120 s of the heating cycle. Here the width that is plotted is the standard deviation of the Gaussian fit to the diffraction peak, which includes the Cu shoulder that appears on the low d-spacing side of the Au peak. Each of the three annealing temperatures behave in a similar fashion whereby the peaks initially narrow, then spike in width before settling down to a width that slowly decreases with increasing annealing time. The initial decrease in peak width, beginning at approximately t=20 s, is most likely caused by the annealing of residual stresses in the initial thin films. This type of decrease in peak width is commonly observed, and is seen here before any measurable diffusion has occurred. The spike in the peak widths, beginning at approximately t=30 s, occurs as the Cu-rich shoulder begins to develop as Cu diffuses into the Au layer as detailed earlier in Fig. 6 for the sample held at 800ºC. At the end of the spike, a somewhat homogeneous Au/Cu layer has formed into a single peak. This homogeneous Au/Cu

layer is enriched in Au relative to the moderately thick Cu layer below it, and its diffraction peak continues to shift with increased annealing time as these two layers interdiffuse. Note that the diffraction peak during the 900ºC annealing temperature was interrupted by a sudden change in texture from an Au(111) preferred orientation to an Au(200) orientation, as will be discussed later.

During the initial stages of diffusion, the diffusion coefficient can be estimated at each temperature as the Cu diffuses through the Au layer of known thickness using the thin-film planar diffusion solution to the diffusion equation. This relationship relates the diffusion distance, X, to the diffusion coefficient, D, and the diffusion time, t, through the well known relationship: $X^2 = 4Dt$ [18]. Taking the diffusion distance to be the thickness of the Au layer, and the diffusion time to be that required for Cu to diffuse through the Au layer, the diffusion coefficient was calculated for each temperature. Here, the diffusion time is assumed to be the amount of time that the spike in the peak width curve exists between its minimum value before the spike begins and the time that this same peak width is observed after the spike has disappeared.

Table 1 summarizes the results of the diffusion calculations for the three annealing temperatures. These data should be taken as a lower bound on the diffusion coefficient since the layer thickness is continuously increasing. Using this approach, the calculated diffusion coefficient is shown to vary from $5.1 \times 10^{-2} \mu m^2/s$ to $2.1 \times 10^{-1} \mu m^2/s$ over the 700ºC to 900ºC temperature range. These data can be compared to reported values of the bulk diffusion coefficient for Au in Cu, which ranges from $5.8 \times 10^{-4} \mu m^2/s$ to $3.8 \times 10^{-2} \mu m^2/s$, and for Cu in Au, which ranges from $7.8 \times 10^{-3} \mu m^2/s$ to $2.8 \times 10^{-1} \mu m^2/s$ over the same temperature range [17]. Thus the difference between the bulk and the thin film diffusion coefficients decreases as the

temperature increases, and the thin film diffusion coefficient is closer to that of Cu in Au than visa versa.

Taking the expression $D=A \exp(-Q/RT)$ to represent the diffusion coefficient [19], the activation energy, Q, and the frequency factor, A, can be determined by plotting the diffusivity data presented in Table 1 as ln(D) versus (1/T) in order to linearize the diffusion expression. This result is presented in Fig. 8 where the slope of the curve is equal to Q/R and the intercept is equal to ln(A). A linear regression through the three data points has an r^2 fit value of 0.973, and gives the activation energy for diffusion of Q=65.4 kJ/mole, and the frequency factor of $A=163 \mu m^2/s$.

Reported values of the activation energies for diffusion of Au into Cu, and Cu into Au, vary considerably. Bulk diffusion measurements indicate that the activation energy for interdiffusion of Au into Cu is 197.8 kJ/mole, $D_{Au/Cu}=0.243 \exp(-197.8/RT)$ (cm^2/s), while that of Cu into Au is 170 kJ/mole, $D_{Cu/Au}=0.105 \exp(-170.0/RT)$ (cm^2/s) [17]. These activation energies are considerably higher than the observed values in the thin films measured in this study, and a comparison of the calculated bulk interdiffusion measurements for Au and Cu with the thin film results is presented in Fig. 8. This comparison shows that the bulk diffusivity of Cu into Au is about 10 times greater than that of Au into Cu at these temperatures. At 900ºC (1000/T(K)=0.85), the bulk diffusivity of Cu into Au is approximately equal to that measured for thin films. However, at lower temperatures where grain boundary diffusion plays a larger role, the measured diffusivity in the thin films is much more rapid. Therefore, based on the low activation energy for interdiffusion measured in the thin films and the high diffusivities at low temperatures, it is apparent that grain boundaries, and/or other defect structures, are playing an important role in diffusion that occurs in the thin films.

It is known that grain boundary diffusion is reported to occur with activation energies that that can be less than bulk diffusion by a factor of 2 or more [7-9]. One study measured the activation energy for grain boundary diffusion of Au in high purity polycrystalline copper at temperatures up to 763ºC to be 81.2 kJ/mole [8]. This activation energy is similar to the measured activation energy of 65.4 kJ/mole found in this study on thin films. Since sputtered thin films are known to form with high amounts of defects and grains growing in columnar fashion along the direction of deposition [9], it is not surprising to see a high fraction of grain boundaries or other defects contributing to the overall diffusion in the Au thin film.

Later Stages of Diffusion

At longer annealing times, long range diffusion creates a Au/Cu layer of unknown thickness that increases with time. It is not straightforward to extract diffusion rates from the time-dependence of these diffraction profiles since the composition varies continuously through the film. Modeling the evolution of the compositional profile would require knowledge of the diffusion rates for both Au and Cu for the full range of Au/Cu solid solutions. A further complication is the large difference in x-ray penetration depth between Au- and Cu-rich material which changes the depth sampled by the beam as interdiffusion progresses.

For these reasons, this work focuses mainly on extracting the activation energy of diffusion at longer times. This suggests making the assumption that interdiffusion can be approximated by a single activation energy, so the evolution of the compositional profile, and therefore the diffraction pattern, at each temperature is similar, and differs only by an overall Arrhenius scale factor in the rate: $I(d,t,T) = f[d, t\exp(Q/RT)]$, where I is the diffracted intensity, d the d-spacing, t time, Q the activation energy, and T the temperature. This assumption allows Q to be found without performing the complex modeling necessary to

determine the function *f* by comparing the time required to reach various stages in the evolution of *I*.

The x-ray diffraction measurements showed that the peaks sharpened with increased annealing time, indicating that a uniform composition is developing in the near surface region. The rate at which this composition evolves can be used as another measure of the activation energy for longer diffusion times. Assuming Vegard's law applies to this system, the lattice parameter of the binary Cu/Au phase will follow a rule-of-mixtures relationship with the atomic fraction of the diffusing elements [16]. Although this law is not always followed, it is a reasonable assumption for the Au/Cu system where deviations from it are on the order of 5% or less [20]. Using Vegard's law the composition of the intermixed Au/Cu phase can be estimated from its measured lattice parameter, and can be expressed by the following equation:

$$X_{Cu} = (a^{o}_{Au} - a^{o}_{Au\text{-}Cu}) / (a^{o}_{Au} - a^{o}_{Cu}) \qquad \text{(eq. 1)}$$

In this expression, X_{Cu} is the atomic fraction Cu in the mixed Au/Cu phase, a^{o}_{Au} is the temperature dependent lattice parameter of Au, a^{o}_{Cu} is the temperature dependent lattice parameter of Cu, and $a^{o}_{Au\text{-}Cu}$ is the measured lattice parameter of the mixed Au/Cu phase as determined by the in-situ x-ray diffraction experiments. The temperature dependent lattice parameters are used here because some transformation was observed to occur during the experiments before the isothermal annealing temperatures were reached.

The x-ray data was analyzed using eq. 1 to determine the composition of the intermixed phase based on the fcc (200) diffraction peaks as a function of annealing time. Figure 9 plots the results for each of the three temperatures up to a total time of 10,000 s, showing the increase in Cu content with annealing time. As expected, the sample held at 900ºC intermixes more rapidly

than the samples held at lower temperatures, and all the samples show a decreased rate of intermixing with increased annealing time. The 700ºC sample was held for a total time longer than is shown in Fig. 9, eventually reaching a fraction Cu of 0.76 at 28,000 s which is similar to that observed in the samples held at the higher temperatures for shorter times. At longer times the Au/Cu diffraction peaks for all three temperatures continue to move to lower d-spacings as interdiffusion continues.

The time required to reach a given composition of the intermixed phase was determined from the results presented in Fig. 9 for several different compositions and for each of the three temperatures using the Au/Cu (200) peaks. These results are presented in Fig. 10, which plots the natural log time versus 1/T for compositions ranging from 0.5 Cu to 0.75 Cu. As before, the slope of this line is related to the activation energy for interdiffusion, and it is clear that activation energies increase with diffusion time. At a Cu fraction of 0.75, the calculated activation energy is 111.4 kJ/mole, which is nearly twice that of the initial diffusion rate. This activation energy falls somewhere between grain boundary and bulk diffusion, indicating that the effects of grain boundaries and defects are decreasing as the interdiffusion becomes more complete. This effect could be caused by grain growth, which would reduce the amount of grain boundary area available for diffusion, or by the saturation of grain boundaries and other defects by interdiffusion.

Note that the diffusion times for the 900ºC temperature at lower amounts of interdiffusion do not fit the 111.4 kJ/mole trend of the remainder of the data, and appear to require longer times to reach a given amount of intermixing. This result is most likely due to the partial melting of the near surface region that occurred in this sample at an early portion of the 900ºC hold. The partial melting and resolidification increased the grain size of the Au film, thus decreasing the overall diffusivity in this sample.

Characterization of the films

Scanning electron microscopy (SEM) was performed on the surface of the films, both before and after annealing, to determine if the grain boundary structure could be determined. Figure 11 compares micrographs of the as-received Au surface to those after 700ºC and 900ºC annealing runs. This surface of the as-deposited Au film (Fig. 11a) has some grooved areas that are on the order of 10 microns or smaller, which most likely correspond to grain boundaries carried through the film from the original stainless steel substrate. Within these larger grains, there are features on the order of 1 micron or smaller which most likely correspond to columnar grains of the as deposited films which are expected in low temperature deposited thin films [9]. Figure 11b shows the structure of the Au surface after annealing for 8 hours at 700ºC. T size of the visible surface features appears to be on the order of 2 microns or less, which appears larger than that of the as deposited film. The sample annealed at 800ºC for 2 hours looked very similar to the sample held at 700ºC for 8 hours, and is not shown here.

In contrast to the samples annealed at 700ºC and 800ºC, the sample annealed at 900ºC shows visible grain boundaries with grain sizes in excess of 20 microns. This microstructure is shown in Fig. 11c, and is pitted with pores up to 1 micron in diameter that are distributed throughout the grains. In addition, the microstructure shows a lath type substructure throughout the grains that appear to have a crystallographic orientation relationship to the grains. At 900ºC, which is near the melting point minimum in the Au-Cu system, diffusion is rapid, allowing the microstructural changes to rapidly occur. Looking over the individual diffraction patterns for this run showed that there was a dramatic change in texture when the temperature first reached its 900ºC set point. Three consecutive diffraction patterns show this transition in Fig. 12. Frame 19 corresponds to a time of 54s after the start of the experiment, just before the sample reaches

900ºC, while frames 20 and 21 correspond to times of 57s and 60s respectively. Due to thermal overshoot of the temperature controller, the temperature of the sample spiked to 918ºC in frame 20, before coming back down to 900ºC for the remainder of the experiment. Since the Au/Cu system has a melting point minimum of 910ºC for a 20wt%Cu composition [10], it is likely that the sample experienced some degree of melting in the diffuse Au/Cu interface. This melting would explain the broad diffraction pattern seen in frame 20 and would help to explain the rapid change in texture of the sample.

A metallographic cross section was made through the sample heated to 800ºC to examine the microstructure of the Au/Cu intermixed zone after annealing. The SEM micrograph of this cross section is shown in Fig. 13, indicating that substantial porosity has developed in the near surface region of the sample. The porosity has a wide size distribution, from less than 100 nm to 500 nm, and appears to be scattered randomly throughout the top 4-5 μm region of the sample. The origin of this porosity is most likely due to the Kirkedall effect [16] that results from the different diffusivities of Cu in Au. The different diffusivities causes a net flux of atoms across a given lattice plane, causing the creation and annihilation of vacancies. Under non-equilibrium conditions, high vacancy concentrations can be generated and cause the precipitation and growth of microvoids which eventually create pores of considerable size, such as those indicated in Fig. 13.

In summary, the thin films appear to have initial columnar grain sizes on the order of a micron or smaller, which results in a high concentration of grain boundaries that accelerate the diffusion kinetics. These grains appear to coarsen at annealing temperatures of 700ºC and 800ºC, which may contribute to the increased activation energy for diffusion at longer annealing times. In addition, Kirkendall voids were observed at these annealing temperatures as a result of the different diffusivities of Au and Cu. At 900ºC, a momentary partial melting of the sample

created much larger grains and visible voids on the surface of the sample. The larger grains appear to have slowed the interdiffusion kinetics of this sample relative to what would be expected if the grain growth had not occurred.

Conclusions

1. In-situ synchrotron radiation was successfully used to track the interdiffusion of Au and Cu during annealing of thin films at 700ºC to 900ºC. The difference in the lattice parameters of these two elements allowed the diffraction peaks of each element to be tracked as a function of annealing time.
2. At short annealing times (<60s) the Cu diffused rapidly through the 3.8μm thick Au film. This intermixing was characterized by a low d-spacing shoulder which developed on the Au peak and grew with time. Eventually one diffraction peak was formed as Cu and Au completely intermixed.
3. The activation energy for interdiffusion was calculated for the initial stage of annealing by measuring the time required to diffuse Cu through the Au layer of known thickness. This activation energy was measured to be 65.4 kJ/mole, which is approximately 0.4x that of bulk diffusion and 0.8x that of grain boundary diffusion values. The low activation energy is attributed to the high density of columnar grain boundaries combined with other defects in the thin film microstructure.
4. As interdiffusion proceeds, the Au-rich thin film layer begins to interdiffuse into the Cu layer below. Homogenization of the two layers takes place over long times and can be tracked as the Au-rich peak monotonically moves to lower d-spacings for times longer than 60s. The activation energy for this stage of intermixing was measured to be 111 kJ/mole, which is between the reported values for grain boundary and bulk diffusion. This change in activation

energy is believed to be related to grain growth, which would reduce the amount of grain boundary area available for diffusion, and to the gradual elimination of other defects in the thin films.

Acknowledgments

This work performed under the auspices of the U.S. Department of Energy by UC, Lawrence Livermore National Laboratory, under Contract No. W-7405-ENG-48. Part of the research was sponsored by the U.S. Department of Energy Division of Materials Sciences and Engineering under contract No. DE-AC05-00OR22725 with UT-Battelle, LLC. The UNICAT facility at the Advanced Photon Source (APS) is supported by the U.S. DOE under Award No. DEFG02-91ER45439, through the Frederick Seitz Materials Research Laboratory at the University of Illinois at Urbana-Champaign, the Oak Ridge National Laboratory (U.S. DOE contract DE-AC05-00OR22725 with UT-Battelle LLC), the National Institute of Standards and Technology (U.S. Department of Commerce) and UOP LLC. The APS is supported by the U.S. DOE, Basic Energy Sciences, Office of Science under contract No. W-31-109-ENG-38. The authors express gratitude to Mr. Ron Forman of LLNL for preparing the PVD coatings, and Mr. Edwin Sedillo of LLNL for performing scanning electron microscopy.

References

1. Electronic Materials Handbook, Vol 1, Packaging, edited by L. Abel et al., *ASM International*, 1989.
2. Th. Heumann and Th. Rottwinkel, Measurement of the Interdiffusion, Intrinsic, and Tracer Diffusion Coefficients in Cu-Rich Cu-Au Solid Solutions," *J. Nuclear Materials*, V69-70, p. 567-570, 1978.
3. F. Hartung and G. Schmitz, "Interdiffusion and reaction of metals: The influence and relaxation of mismatch-induced stress," *Phys Rev. B*, Vol 64(24)/245418(13), 2001.
4. K. N. Tu and B. S. Berry," X-ray Study of Interdiffusion in Bimetallic Cu-Au Films," *J. Appl. Phys*, V 43(8), p. 3283, 1972.
5. J. A. Borders, "Ion Back-Scattering Analysis on Interdiffusion in Cu-Au Thin Films," *Thin Solid Films*, V19, pp. 359-370, 1973.
6. A. N. Aleshin, V. K. Egorov, B. S. Bokstein and P. V. Kurkin, "Study of Diffusion in Thin Au-Cu Films," *Thin Solid Films*, V223, pp. 51-55, 1993.
7. T. Surholt and Chr. Herzig, "Grain Boundary Self Diffusion in Cu Polycrystals of Different Purity," *Acta Mater*, V45(9), pp. 3817-3823, 1997.
8. T. Surholt, Yu. M. Mishin, and Chr. Herzog, "Grain-boundary Diffusion and Segregation of Gold in Copper: Investigation in the type-B and type-C kinetic regime," *Phys Rev B*, V50(6), pp 3577-3587, 1994.
9. Milton Ohring, *Materials Science of Thin Films, Deposition and Structure*, 2nd ed, Academic Press, 2002.
10. Binary Alloy Phase Diagrams, Vol 1, 2nd ed, edited by T. B. Massalski, *ASM International*, 1990.
11. J. W. Elmer, J. Klingmann, and K. Van Bibber, "Diffusion Bonding and Brazing of High Purity Copper for the Next Linear Collider," *Physical Review Special Topics—Accelerators and Beams*, Vol. 4, Issue 5, APS, 53502-1 to16, 2001.
12. J. W. Elmer, T. A. Palmer, S. S. Babu and E. D. Specht,"Low Temperature Relaxation of Residual Stress in Ti-6Al-4V," *Scripta Materialia,* v52, pp1051-1056, 2005.
13. J. W. Elmer, T. A. Palmer, S. S. Babu, and E. D. Specht, "In-situ Observations of Lattice Expansion and Transformation Rates of α and β Phases in Ti-6Al-4V," *Materials Science and Engineering A*, 391, pp104-113, January, 2005.

14. A. P. Hammersley, FIT2D V9.129 Reference Manual V3.1, ESRF Internal Report, ESRF98HA01T, 1998.
15. A.P. Hammersley, S.O. Svensson, M. Hanfland, A.N. Fitch, D. Häusermann, *High Pressure Research*, 14, 235-248, 1998.
16. B. D. Cullity and S. R. Stock, *Elements of X-Ray Diffraction*, 3rd Ed, Prentice Hall, Upper Saddle River, NJ, 2001.
17. C. J. Smithells, E. A. Brandes, G. B. Brook. *Smithells Metal Reference Book*, 7th ed, Butterworth-Heinemann Ltd., Oxford, United Kingdom, 1992.
18. P. D. Shewmon, *Diffusion in Solids*, McGraw Hill, 1963.
19. J. W. Christian: The *Theory of Transformations in Metals and Alloys, 2nd Edition, Part I,* 1975, Oxford: Pergamon.
20. C. S. Barrett, *Structure of Metals*, McGraw Hill, 1943.

Table 1: Estimated diffusion coefficients for the three temperatures based on the peak width measurements.

Time to diffuse through Au layer (s)	Temperature (ºC)	Au-film thickness (μm)	D ($\mu m^2/s$)
54	700	3.38	0.053
38	800	3.76	0.093
22	900	4.33	0.213

Figure Captions

Figure 1: a) Schematic of the x-ray setup used for in-situ observations of phase transformations under controlled heating and cooling conditions. b) Photograph of the center section of one of the coated samples, showing the Au layer (25 mm wide) on top of the Cu layer and stainless steel substrate.

Figure 2: Initial diffraction pattern of the gold-coated copper sample at room temperature, showing Deby arcs on the CCD areal detector. The Bragg angle is highest, the d-spacing lowest, and the top of the pattern.

Figure 3: Initial diffraction pattern at room temperature showing 3 sets of diffraction peaks for each of the Au and Cu layers. An additional Au peak appears at the lowest d-spacing.

Figure 4: D-spacings (symbols) for the Au 200 and Cu 200 planes as a function of time for: a) 700 ºC, b) 800 ºC, and c) 900 ºC. The solid lines plot the temperature profile of the sample.

Figure 5: Comparison between the initial and the final diffraction pattern of the sample held at 800°C for 2 hrs. The initial Cu peaks disappear, while the lattice parameter of the Au peaks decrease as indicated by the arrows. Similar changes were observed in the samples held at 700°C and 900°C.

Figure 6: Peak profiles for the (220) reflections taken at 3-s intervals during the 800°C anneal. These profiles show the rapid interdiffusion stage from t=36s to t=57s, where a Cu-rich shoulder builds up and grows on the low d-spacing side of the Au peak, and eventually creates a single Au/Cu peak.

Figure 7: Peak widths versus time for each of the three annealing temperatures. Narrowing of the peaks occurs around t=20s due to annealing. The spike in peak widths corresponds to diffusion of Cu into the Au layer.

Figure 8: Comparison of the initial thin-film diffusion coefficient with reported bulk diffusion values for Au in Cu and Cu in Au (dashed lines). The results of this study (solid line and symbols) for thin films based on the spike in peak widths at early annealing times. Activation energies are in KJ/mole.

Figure 9: Compositions of intermixed phase as a function of annealing time for the three annealing temperatures as determined by shifts in the fcc(200) diffraction peaks.

Figure 10: Plot showing the natural log of the time required to reach Cu compositions ranging from 0.50 to 0.75 for each of the three annealing temperatures. The activation energy indicated is in kJ/mole.

Figure 11: Scanning electron micrographs of the Au surface. A) Prior to annealing, B) after annealing at 700ºC, and 800ºC) after annealing at 900ºC.

Figure 12: Three consecutive x-ray diffraction peaks from the sample heated to 900ºC. These x-

ray patterns show the change in texture from Au(111) to Au(200), and a shift to lower d-spacing as Cu diffuses into the Au layer.

Figure 13: SEM cross section micrograph of the near surface region of the sample annealed at 700ºC. Kirkendall voids appear in a zone of thickness similar to that of the initial Au layer.

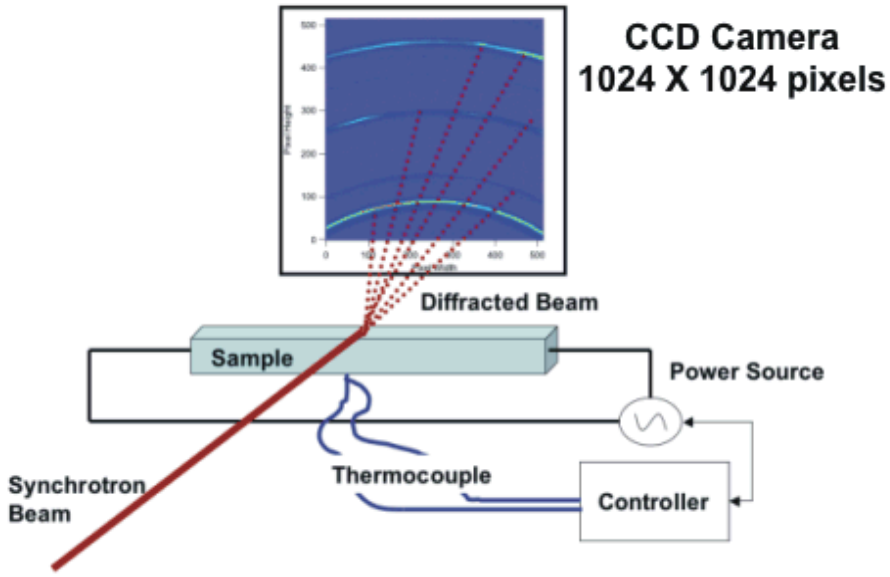

a)

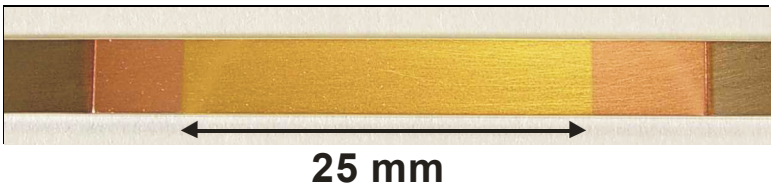

b)

Figure 1: a) Schematic of the x-ray setup used for in-situ observations of phase transformations under controlled heating and cooling conditions. b) Photograph of the center section of one of the coated samples, showing the Au layer (25 mm wide) on top of the Cu layer and stainless steel substrate.

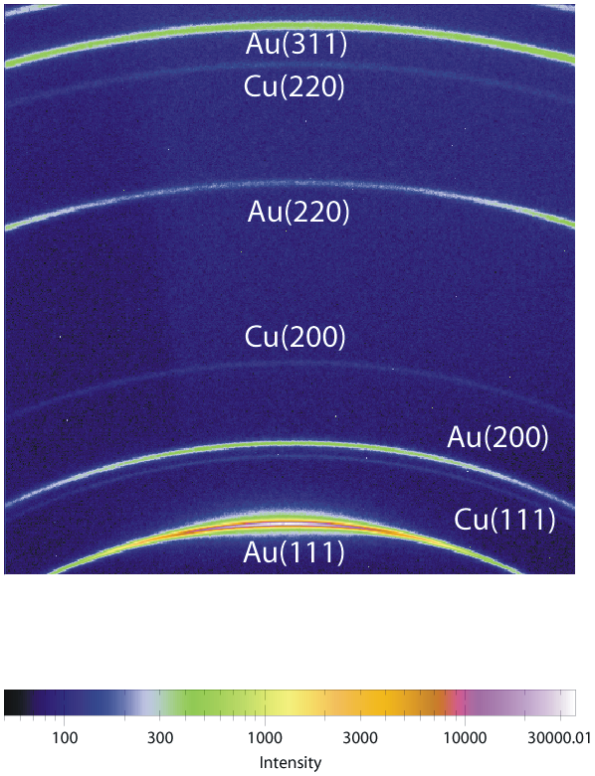

Figure 2: Initial diffraction pattern of the gold-coated copper sample at room temperature, showing Deby arcs on the CCD areal detector. The Bragg angle is highest and the d-spacing lowest at the top of the pattern.

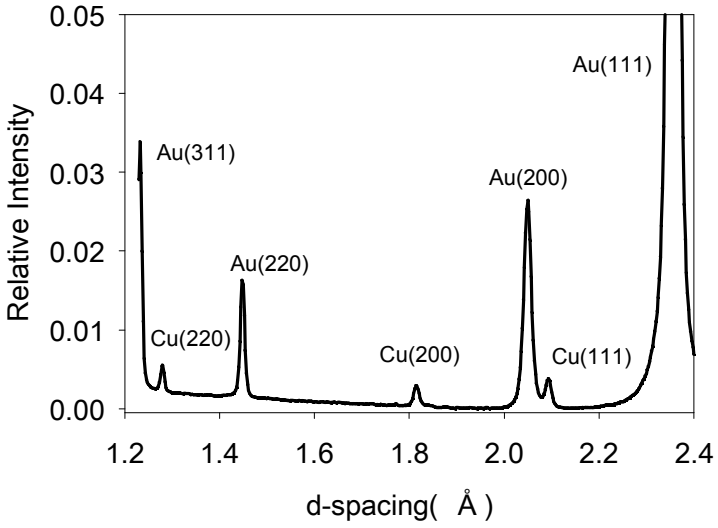

Figure 3: Initial diffraction pattern at room temperature showing 3 sets of diffraction peaks for each of the Au and Cu layers. An additional Au peak appears at the lowest d-spacing.

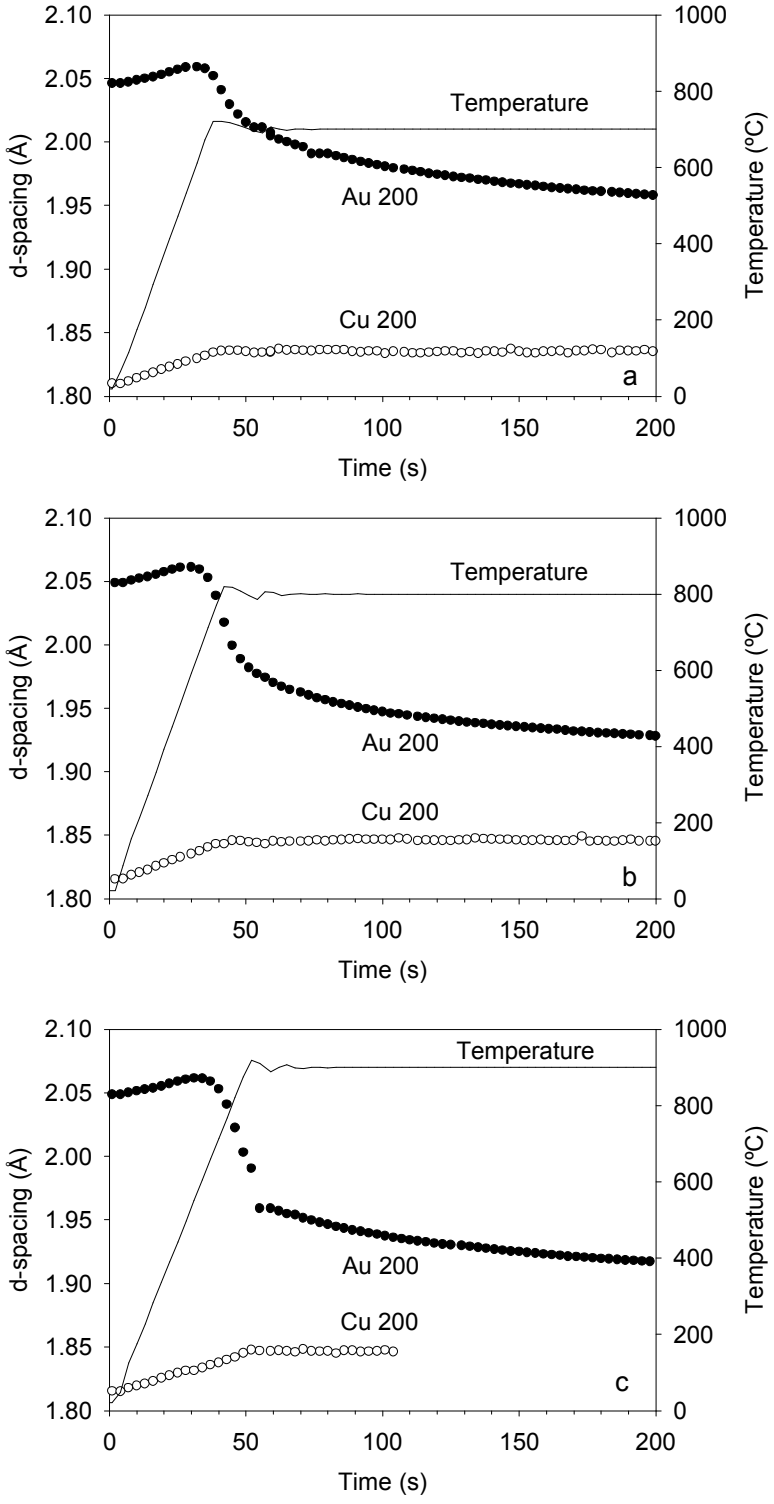

Figure 4: D-spacings (symbols) for the Au 200 and Cu 200 planes as a function of time for: a) 700 ºC, b) 800 ºC, and c) 900 ºC. The solid lines plot the temperature profile of the sample.

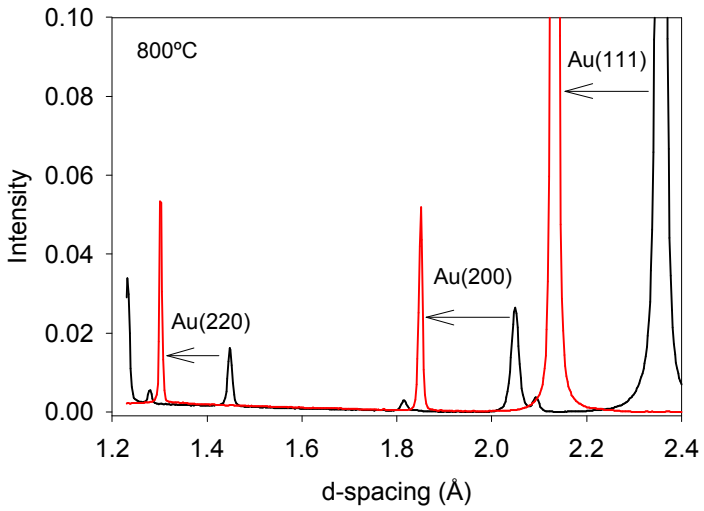

Figure 5: Comparison between the initial and the final diffraction pattern of the sample held at 800°C for 2 hrs. The initial Cu peaks disappear, while the lattice parameter of the Au peaks decrease as indicated by the arrows. Similar changes were observed in the samples held at 700°C and 900°C.

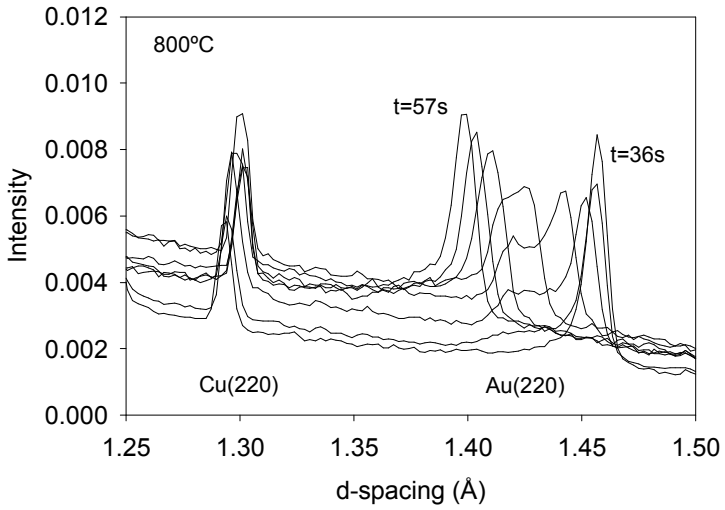

Figure 6: Peak profiles for the (220) reflections taken at 3-s intervals during the 800°C anneal. These profiles show the rapid interdiffusion stage from t=36s to t=57s, where a Cu-rich shoulder builds up and grows on the low d-spacing side of the Au peak, and eventually creates a single Au/Cu peak.

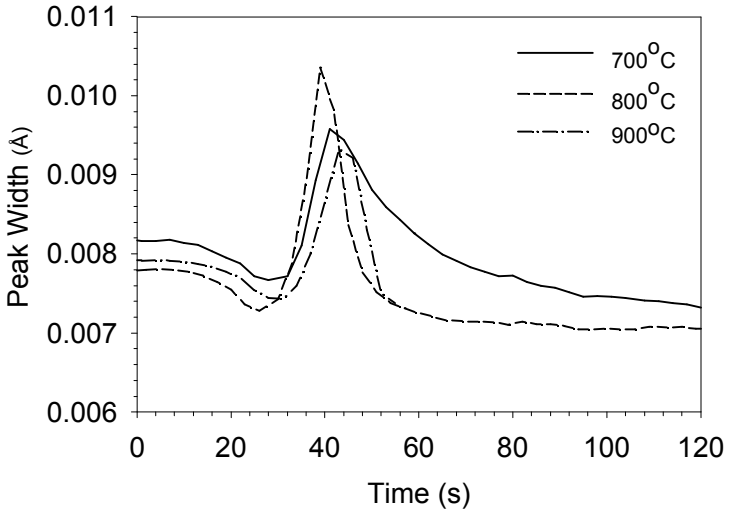

Figure 7: Peak widths versus time for each of the three annealing temperatures. Narrowing of the peaks occurs around t=20s due to annealing. The spike in peak widths corresponds to diffusion of Cu into the Au layer.

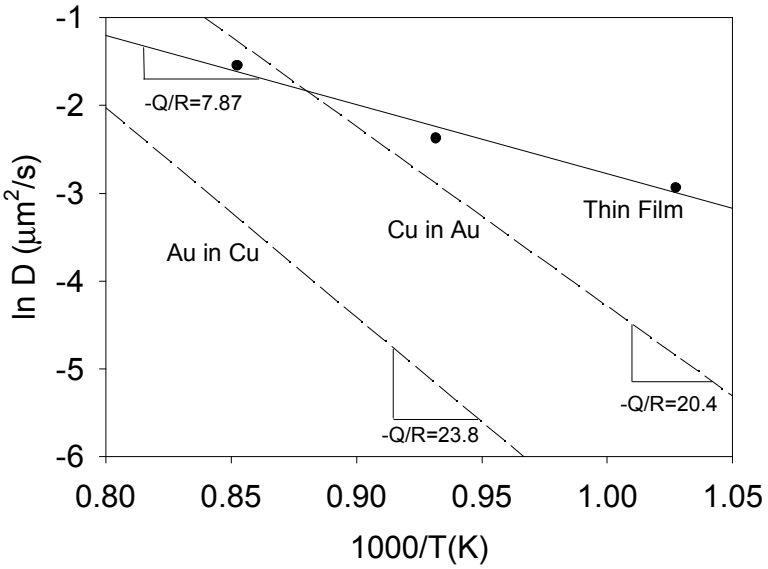

Figure 8: Comparison of the initial thin-film diffusion coefficient with reported bulk diffusion values for Au in Cu and Cu in Au (dashed lines). The results of this study (solid line and symbols) for thin films based on the spike in peak widths at early annealing times. Activation energies are in KJ/mole.

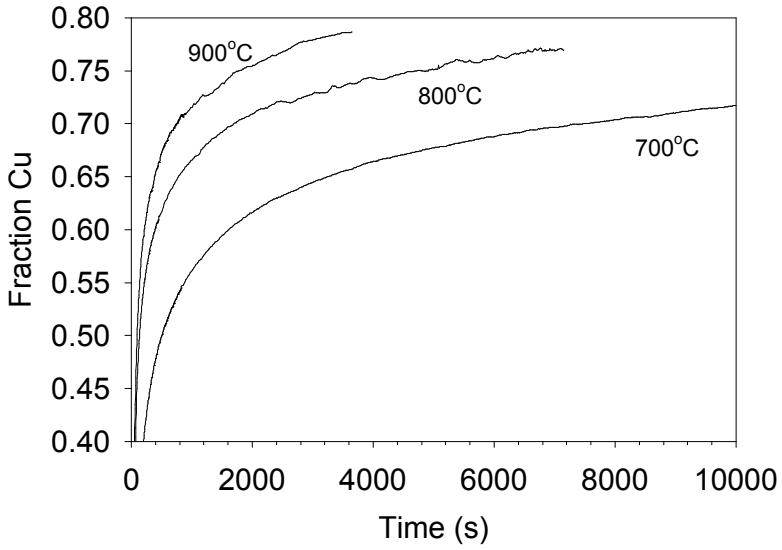

Figure 9: Compositions of intermixed phase as a function of annealing time for the three annealing temperatures as determined by shifts in the Au/Cu(200) diffraction peaks.

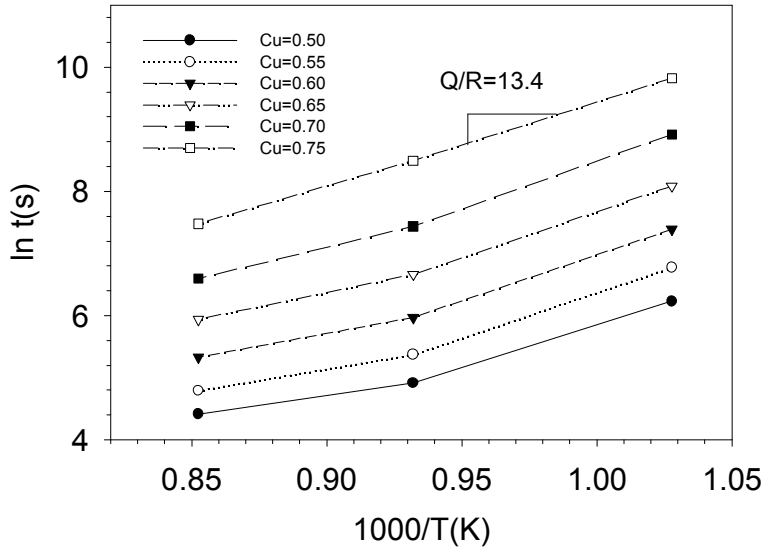

Figure 10: Plot showing the natural log of the time required to reach Cu compositions ranging from 0.50 to 0.75 for each of the three annealing temperatures. The activation energy indicated is in kJ/mole.

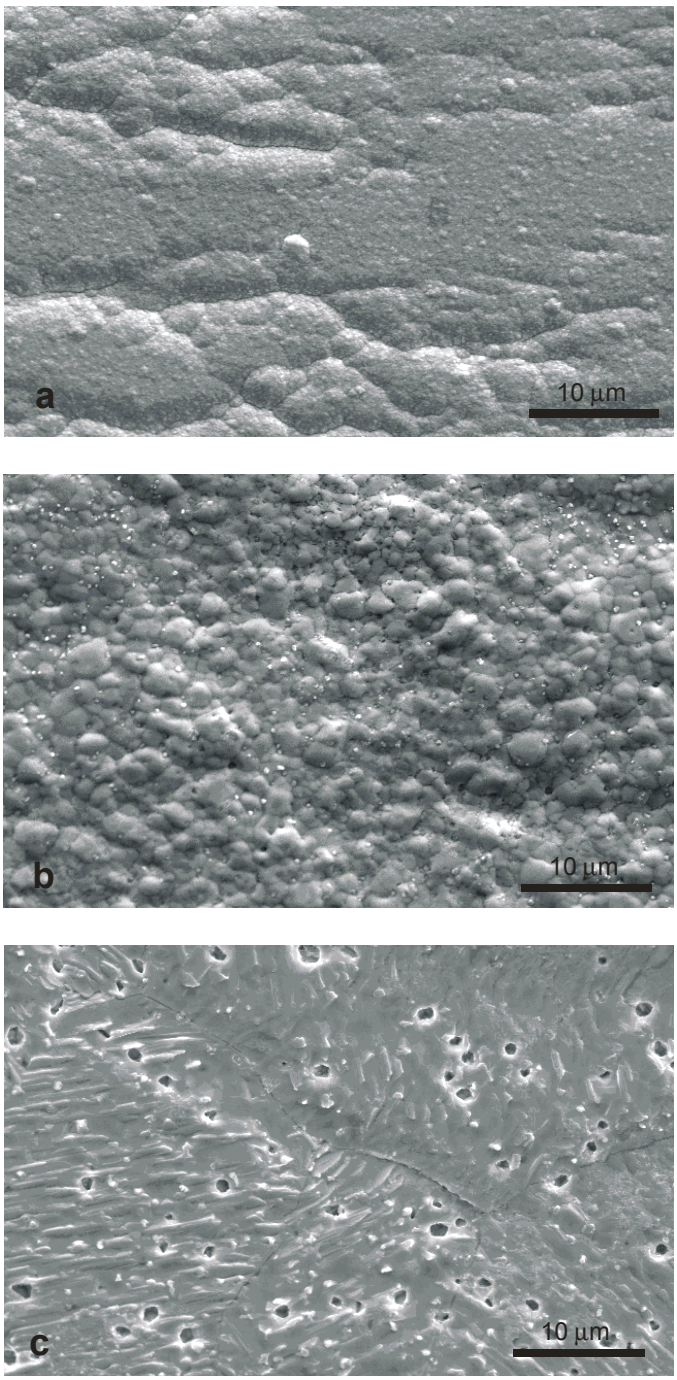

Figure 11: Scanning electron micrographs of the Au surface. A) Prior to annealing, B) after annealing at 700ºC, and C) after annealing at 900ºC.

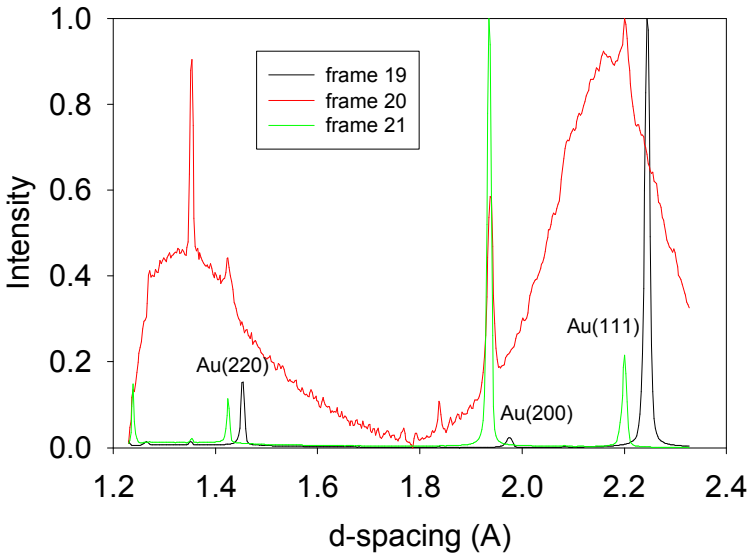

Figure 12: Three consecutive x-ray diffraction peaks from the sample heated to 900ºC. These x-ray patterns show the change in texture from Au(111) to Au(200), and a shift to lower d-spacing as Cu diffuses into the Au layer.

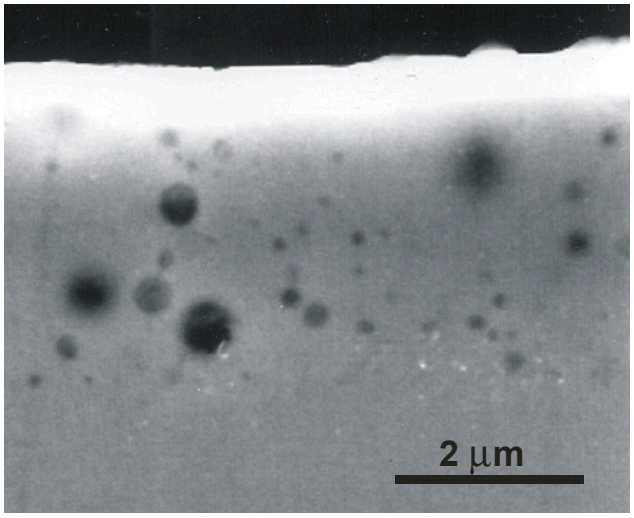

Figure 13: SEM cross section micrograph of the near surface region of the sample annealed at 700ºC. Kirkendall voids appear in a zone of thickness similar to that of the initial Au layer.